EM Design of an Isolated Coplanar RF Cross for MEMS Switch Matrix Applications

W.Simon [1], A.Lauer [1], B.Schauwecker [2], A.Wien [1]

1 IMST GmbH, Carl-Friedrich-Gauss-Str. 2, 47475 Kamp Lintfort, Germany; E-Mail: simon@imst.de
2 DaimlerChrysler AG, Research & Technology, Wilhelm-Runge-Strasse 11, 89081 Ulm, Germany

The EM design of a Coplanar RF Cross with well isolated signal paths in a frequency range from DC up to 40 GHz is described. The cross is designed for a MEMS switch matrix where the different signal paths have to be isolated against each other. This allows to have several 'on-state' signal paths at the same time in the matrix. One signal path is routed via an underpath metallisation while the other signal path is routed with an air bridge. A metal sheet connecting both coplanar ground metallisations is used as a shield to achieve good isolation. The optimisation of all elements from the cross is done with a full wave FDTD simulator.
The achieved isolation between the two signal paths of the coplanar RF cross is above 40 dB up to 40 GHz. For both signal paths is in measurement and simulation for frequencies up to 20 GHz the return loss better than 18 dB and the insertion loss is below 0.7 dB.

I. INTRODUCTION

Many microwave and mm-wave applications like radar systems or communication systems have a switch matrix included in their components. The losses in this matrix can be significantly reduced if MEMS switches are used instead of standard PIN diode switches [1]. The isolated RF coplanar cross described in this paper increases the flexibility in the signal routing of the matrix as several signal paths can be at the same time at 'on state'.

II. RF CROSS DESIGN

The design of the RF cross has been performed by 3D electromagnetic field simulations. These simulations necessarily include all 3D coupling effects between the two signal paths and the substrate. The simulation program EMPIRE™ [2] has been used. It is based on the Finite Difference Time Domain (FDTD) method [3,4] and allows efficient and accurate simulation of MEMS components [5].

A. Generic RF Cross

The RF cross is designed for a coplanar environment on high-resistivity silicon wafers (> 4000 Ωcm) with a wafer thickness of 525 µm. The center conductor width is 144 µm and the width of the gap width is 78µm for a 50 Ω coplanar line. In the area of the cross is the center conductor of the coplanar line routed from one signal path via a 300 nm thin underpath metallisation below the center conductor of the crossing coplanar line (see Fig. 1). The center conductor of the upper coplanar line is created as a high air bridge to be able to cross the ground conductor in the area of the cross. Due to this high air-bridge is, compared to a standard air bridge, a larger distance between the two signal lines achieved, which increases the isolation between both signal paths. Both ground connections of the crossing line are connected via air bridges.

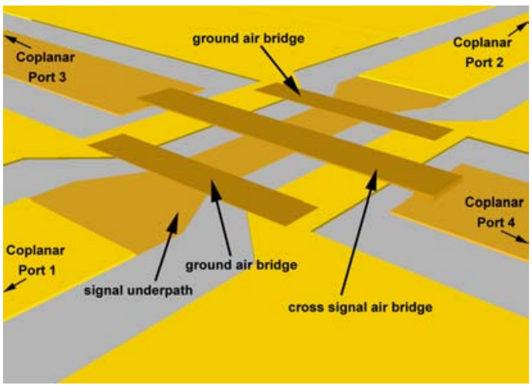

Fig. 1: 3D view of the generic RF cross (simulation model).

In the area of the cross the ground-to-ground width of the coplanar line is reduced to obtain shorter air bridges. A reduced width of the centre conductor creates again a 50 Ω line.

The simulation results of this generic RF-cross are shown in Fig. 2.

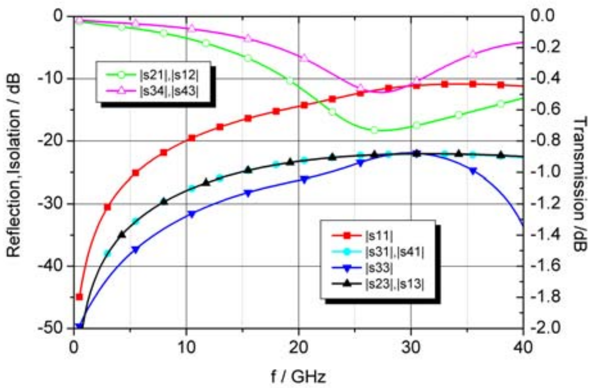

Fig. 2: Simulation results of the RF cross.

The isolation is between both ports for frequencies up to 40 GHz above 22dB. The signal path between port one and port two has a return loss below 11 dB. This and the high insertion loss of up to 0.6 dB is caused by the crossing ground- and signal-air-bridges. They build a capacitive load to the 50 Ω coplanar line. A compensation of these capacities could be achieved by series inductivities at both sides of the cross combined with a changed coplanar linetype in this area (see part *B*). The crossing signal path's return loss is above 22 dB and the insertion loss is below 0.45 dB.
The magnitude of the electric field at 20 GHz in the plane of the crossing signal bridge, while the straight signal path is excited, is shown in Fig. 3.

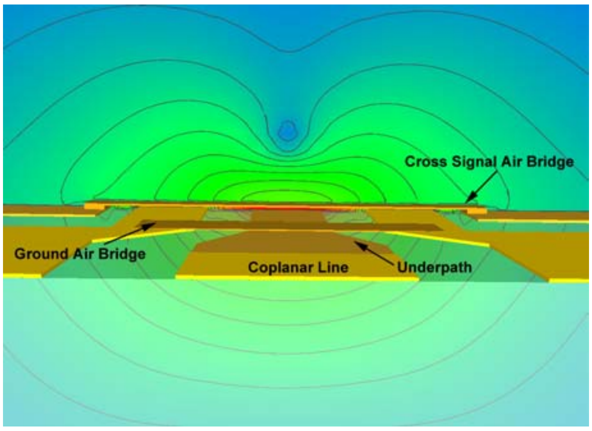

Fig. 3: Magnitude of electric field at the straight signal path at 20 GHz.

The field strength is indicated by colour from red (high field values) to blue (low field values) with a difference of 50 dB in between. Lines of the same field strength are shown in grey. It can be seen that the highest field values are between the underpath signal line and the crossing signal path air bridge. The scattering field is above and inside the substrate quite large and covers a large area of the crossing signal path, which creates the coupled signal to the ports 3 and 4.

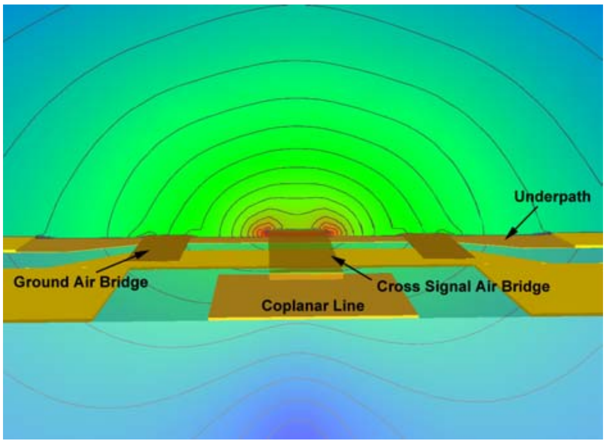

Fig. 4: Magnitude of electric field at the crossing signal path at 20 GHz.

The magnitude of the electric field at 20 GHz in the plane of the straight signal path, while the cross signal path is excited, is shown in Fig.4. The highest field values are between the cross signal air bridge and the underpath and at the edges of the air bridge. The main part of the scattering field reaches a long distance of the straight signal path from the top, while the scattered field is not so strong in the substrate.

B. Optimised isolated RF Cross

The generic RF cross described in *A* has been optimised to increase the isolation between the two signal paths. A first point is the reduction of the ground-to-ground spacing of the coplanar line from 300 µm to 110 µm. This reduces the effective field width of the coplanar line and allows the use of a shorter air-bridge. Both effects reduce the coupling between the two signal paths. In addition the production of these shorter air-bridges is easier yielding better the reliability of the structure. The modified RF cross together with a visualisation of the magnitude of the magnetic field at 20 GHz, for the case that the straight signal path is excited, is shown in Fig. 5. It can be seen that the scattering field is now concentrated in a smaller area above and below the underpath line.

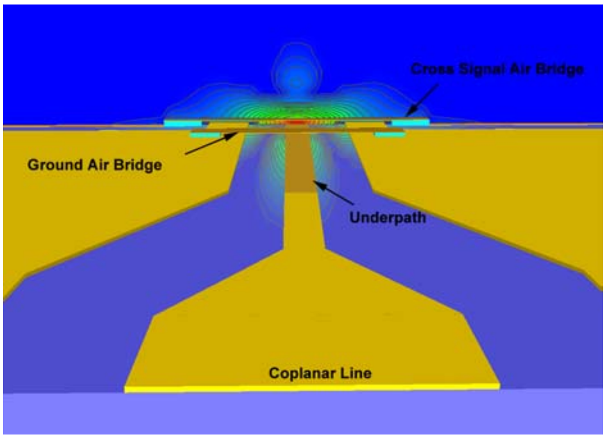

Fig. 5: Magnitude of electric field at the straight signal path at 20 GHz for the optimised RF cross.

The magnitude of the electric field at 20 GHz in the plane of the straight signal path, while the cross signal path is excited, is shown in Fig.6. It can be seen that the main field is located between the cross signal air bridge and the underpath line and at the edges of the air-bridge. The scattered field is much weaker compared to the generic RF cross.

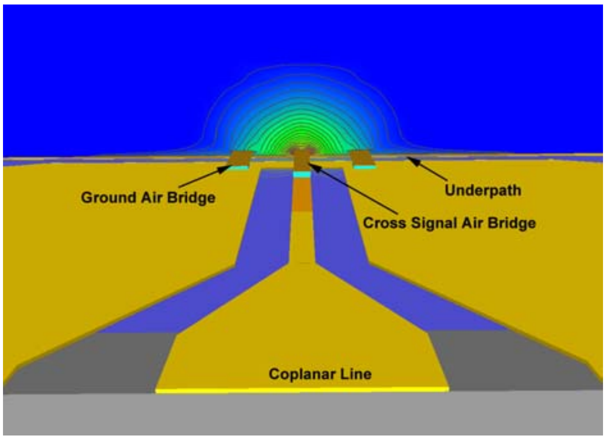

Fig. 6: Magnitude of electric field at the crossing signal path at 20 GHz for the optimised cross.

A further improvement of the isolation could be achieved by preventing a direct coupling between the two signal paths. This is realised by introducing a lower shielding air-bridge (see Fig.8, orange sheet) connecting both ground metallisations between the underpath signal line and the upper cross signal air-bridge. The outside coupling through the air has been reduced with upper shielding air bridges connecting the ground metallisations in a larger area around the cross (600 µm x 600 µm). An overlap of 10µm between the two shielding air bridges prevents leaking radiation from the underpath to the cross signal air bridge. A comparison of the isolation between the two signal paths for the three RF cross designs is shown in Fig. 7. The isolation between the two signal paths of at least 22dB for a frequencies up to 40 GHz at the generic RF cross could be increased above 30 dB for the RF cross with the reduced ground to ground spacing.

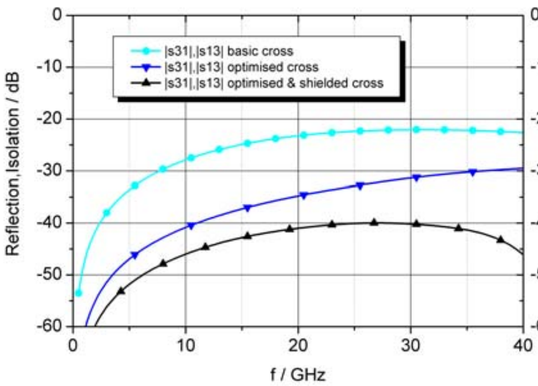

Fig. 7: Isolation between the two signal paths at the different RF cross designs.

The shielding air bridges which are introduced in the final RF cross design (see Fig. 8) increase the isolation between the two signal paths for frequencies up to 40 GHz above 40 dB.

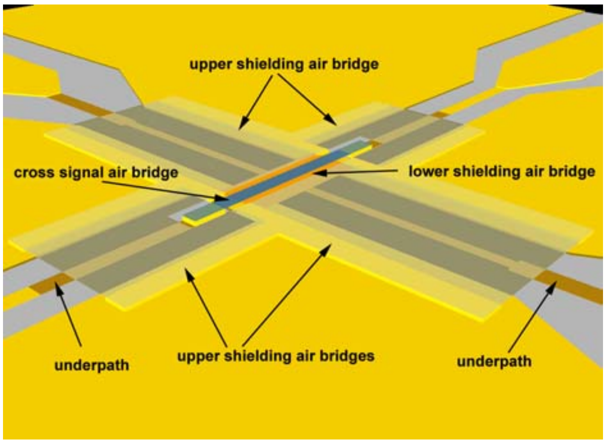

Fig. 8: 3D view of the final RF cross design

Due to the shieldings the field of the underpath signal line is concentrated below the shielding bridges and in the substrate. The field from the crossing signal line is concentrated mainly above the upper shielding bridge and in the air (see Fig. 9 and 10).

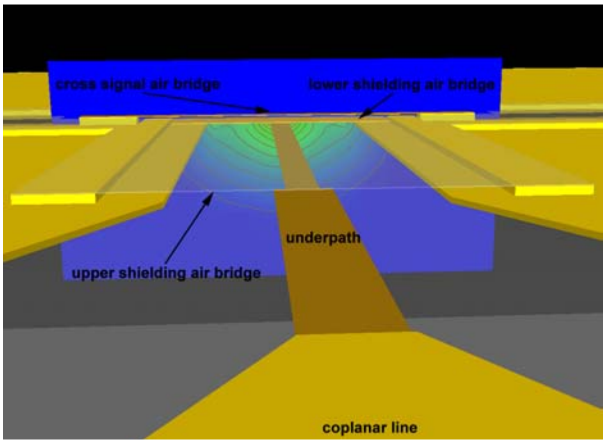

Fig. 9: Magnitude of electric field at the underpath at 20 GHz for the final RF cross design

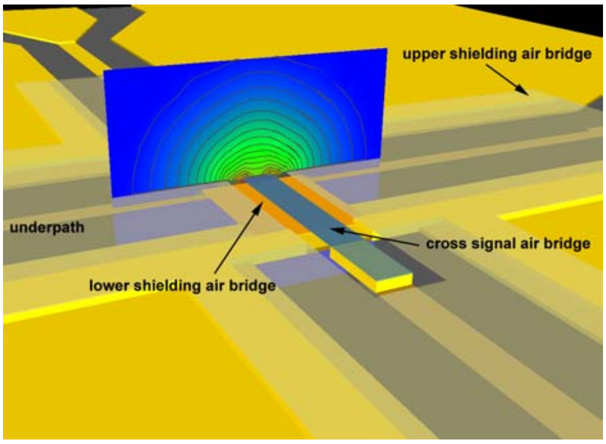

Fig. 10: Magnitude of electric field at the underpath at 20 GHz for the final RF cross design

For an optimisation of the RF performance the small centre conductor lines have been designed to create a microstrip mode against the shielding electrodes with an impedance near 50 Ω. Short inductive lines are used for compensation outside the shielded area. The simulation and measurement results of the RF cross show an excellent performance (see Fig. 11). The return loss is in the simulations better than 20 dB for frequencies up to 35 GHz for both signal paths while the measurements show a return loss better that 17 dB. The insertion loss is for the crossing signal path 0.5 dB for frequencies up to 20 GHz while the underpath has an insertion loss of 0.8 dB. This is founded in the longer underpath line, which has due to the thickness of 300 nm higher losses than the standard CPW line. The isolation between the two signal paths is in the simulations above 40 dB for frequencies up to 35 GHz.

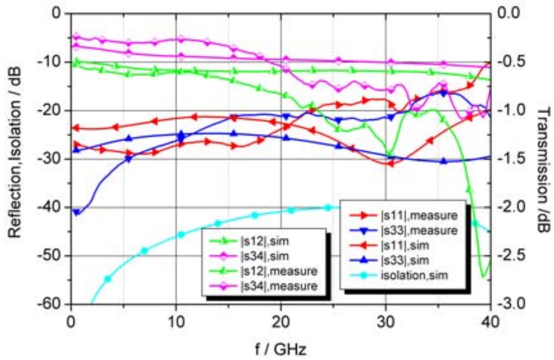

Fig. 11: Simulation and measurement results of the RF cross.

III. CONCLUSION

A new RF Cross design is presented. It shows excellent broadband performance regarding isolation between the two signal paths. This offers the potential for building new compact switching matrices with a high freedom in the signal routing.

IV. ACKNOWLEDGEMENT

The authors would like to acknowledge K.M. Strohm and J.-F. Luy (DaimlerChrysler AG, Research & Technology Ulm,) for fruitful discussions. Partial funding by ESA/ESTEC, Contract No. 14547/00/NL/CK, is gratefully acknowledged.

V. REFERENCES

[1] B. Schauwecker, K. M. Strohm, W. Simon, J. Mehner, J.-F. Luy, " Toggle-Switch - A new type of RF MEMS switch for power applications"; IMS2002, pp. 219-222,Seattle , USA, June 2002

[2] IMST GmbH, "User and Reference Manual for the 3D EM Time Domain Simulator Empire", http://www.empire.de/empire.pdf, June 2002

[3] K. S., Yee: "Numerical solution of initial boundary value problems involving Maxwell's equations in isotropic media." *IEEE Trans. Antennas and Propagation.* Vol. AP-14, S. 302-307, 1966

[4] Allen Taflove "Computational Electrodynamics: The Finite-Difference Time-Domain Method", Artech House, Norwood, MA, 1995

[5] W.Simon, B.Schauwecker, A.Lauer, A.Wien: "Designing a novel RF MEMS switch for broadband power applications", European Microwave Conference, pp.519-522, Mailand, September 2002